

Raman study of water deposited in solid argon matrix

Vlasta Mohaček-Grošev^{a†}, Krešimir Furić^b and Vedran Vujnović^c

^a Center of Excellence for Advanced Materials and Sensing Devices, Research Unit New Functional Materials, Ruđer Bošković Institute, Bijenička 54, 10000 Zagreb, Croatia, Vlasta.Mohacek.Grosev@irb.hr

^b Ruđer Bošković Institute, Bijenička 54, 10000 Zagreb, Croatia, kfuric@gmail.com

^c Department of Physics and Centre for Micro- and Nanosciences and Technologies, University of Rijeka, Radmile Matejčić 2, 51000 Rijeka, Croatia, vedran.vujnovic@phy.uniri.hr

Abstract

New Raman data are presented concerning H₂O and D₂O water aggregation in argon matrix having the ratio of number of argon atoms to water molecules close to 40:1. Experiments were conducted at temperatures from 8 K to 34 K allowing observation of OH and OD stretching vibrations of water monomers, dimers, trimers and higher multimers, as well as broad bands corresponding to solid amorphous water. Molecular dynamics simulations were performed for thirteen or sometimes fourteen water molecules dispersed among 500 argon atoms. Resulting final configurations included dimers, trimers, tetramers and pentamers, all in open chain configurations which upon optimization resulted in mostly cyclic conformations. Observed OH stretching vibrations were assigned by comparing calculated normal modes in harmonic approximation at the B₃LYP/aug-cc-pVDZ and PBEPBE1/aug-cc-pVDZ level of theory with our data and previously observed bands from infrared matrix isolation studies and Raman jet cooled experiments. Raman bands assigned to water multimers in argon matrix are shifted 20 to 25 cm⁻¹ towards lower wavenumbers with respect to the positions of OH stretching vibrations of almost free water clusters.

Keywords: matrix isolation; water clusters; water oligomers; low temperature spectroscopy; Raman; vibrations; hydrogen bonding; molecular dynamics simulation

Prepared for *Spectrochimica Acta A: Molecular and Biomolecular Spectroscopy*

† Author to whom correspondence should be sent, e-mail: Vlasta.Mohacek.Grosev@irb.hr

Introduction

Water aggregation is crucial for optimal functioning of humans and living beings in general: we need water to sustain life. Be it in the cytosol or in the extracellular matrix [1], in the first hydration shell of proteins or inside pores of intramembrane proteins [2], water molecules perform their role by adjusting their position and number, stretching or rotating, facilitating the optimal performance of enzymatic active sites [3], minimizing the energies of chemical reactions [4], and providing solvation free energies of proteins that are crucial for their performance [5]. Such adaptiveness of water molecules results in an abundance of water solid phases, more than ten crystal phases being reported [6]. In the seminal paper by Linus Pauling, in which he calculated the entropy of ice, he used few assumptions widely applied until today, namely that „each molecule is oriented so that its two H atoms are directed approximately toward two of the four oxygen atoms which surround it tetrahedrally, forming hydrogen bonds“, and that only one hydrogen atom lies approximately along oxygen – oxygen axis of any two neighboring water molecules [7]. According to Teixeira, the short lifetime of the hydrogen bond (of the order of 1 ps) is crucial for liquid water, which would otherwise behave as a gel [8]. While there are infinite number of H-bond configurations present in liquid water, the number of possible clusters for a fixed number of n aggregated water molecules is finite. For dimers to hexamers, vibration-rotation-tunneling work by Keutsch and Saykally [9] and IR vibrational spectra of $H^+(H_2O)_n$ by Headrick et al [10] have provided valuable experimental data, whereas theoretical work by Xantheas and coworkers examined optimal geometries and bonding energies predicted by different density functionals compared to *ab initio* methods [11-13]. A proposal for structuring of water by Martin Chaplin aims to unite many different aspects [14].

Normal modes of vibration of a free water molecule were obtained by solving quantum mechanical Hamiltonian in valence coordinates for the first time by Bonner in 1934. [15]. The fact that water molecule is an asymmetric top having two fundamental O-H stretching vibrations overlapping with the overtone of the H-O-H bending vibration contributes to the complexity of the observed vibration-rotational [16] and rotational energy levels [17] of the vapour. Integrated intensities of the Raman bands of water vapour are two orders of magnitude smaller than the Raman intensity of nitrogen stretching band [17], therefore it comes as no surprise that infrared vibrational studies of water monomer were much more frequent compared to Raman works [17-19]. Water dimer has an electric dipole moment, a plane of symmetry and a nearly linear hydrogen bond between the two oxygen atoms [20,21]. Proton tunneling in water trimer was evidenced by the quadruplet splitting of every rotational line in the vibrational-rotational-tunneling spectrum of water vapour around 89.5 cm^{-1} by Pugliano and Saykally [22]. Huang and Miller reported first rotationally resolved spectrum of $(H_2O)_2$ in the gas phase [23,24], while infrared predissociation spectroscopy [25], supersonic expansion of water clusters in helium jet [26], cavity ringdown spectroscopy [27], and molecular beam depletion spectroscopy [28] experiments have also contributed to our understanding of water multimers.

Matrix isolation experiments as well as jet cooled clusters spectroscopy studying water vibrational spectrum are almost exclusively performed with infrared spectrometers [29-41]. The first article reporting matrix isolation of water in nitrogen was by Van Thiel, Becker and Pimentel in 1957 [29]. As the matrix ratio (number of moles of gas divided by moles of water, M/A) increased, so did the intensities of bands assigned to monomer species, while the bands

whose intensity decreased were assigned to water dimer and other multimers [29]. Glasel isolated water in argon and xenon matrices having the matrix ratio of 600:1 [30]. Forney, Jacox and Thompson used neon for matrix isolation of water and reported vibrational-rotational transitions for H_2^{18}O and H_2^{16}O [31]. Tursi and Nixon continuously varied the matrix ratio between 40 and 400 and assigned to monomer species the bands whose intensity rose with the increase of M/A, the bands whose peaks passed through a maximum at $M/A \sim 70$ were assigned to dimers; finally all bands whose intensities continuously decreased with the increase of M/A were attributed to trimers, tetramers and other multimers [32]. Water trimer was a subject of extensive review article by Keutsch, Cruzan and Saykally [38], in which the study of Engdahl and Nelander on isotopically substituted $(\text{H}_2\text{O})_3$ is discussed [39].

Several *ab initio* and density functional theory (DFT) studies have been taking place simultaneously and in combination with the experimental works over the years [9,38-49]. The stable structures of water trimer, tetramer and pentamer are found to be cyclic [9]. Tetramer, pentamer and hexamer bands were discussed by Ceponkus et al. in relation to their spectra of water trapped in neon, argon and para-hydrogen matrices [40]. Hirabayashi and Yamada studied OH stretching vibrations of water clusters trapped in Ar and Kr matrices and proposed assignments based on previous *ab initio* calculations of $(\text{H}_2\text{O})_n$ vibrations for $n=2-6$ including cyclic, cage and book water hexamers [41]. As the number of water molecules in a cluster rises, so does the number of possible stable cluster configurations. Also, some cluster structures which are found to be stable with one choice of density functional/basis set, are found not to be stable if different calculation method is attempted. E.g. open chain water trimer having C_{2v} symmetry denoted (a,dd,a) by Xantheas [44], is found to be 0.5 kcal/mole higher in energy than the cyclic trimer when MP2/aug-cc-pVDZ/BSSE corrected procedure is undertaken [44], while it was not listed as a stable structure by Day et al. who used PM3 followed by HF/6-31G* and G3 model chemistry [45]. On the other hand, M6 et al. found three stable trimer structures, one cyclic and two open chain ones, at the MP2/6-311++G(2d,2p) level of theory [46]. Various density functionals were benchmarked for calculating dipole polarizabilities of water clusters having $n = 2-12$ by Hammond et al. [12]. Their conclusion was that for monomer the role of basis set was more important than that of electron correlation. For multimers it was determined that PBE0 density functional with aug-cc-pVDZ basis set produces overall remarkably accurate polarizabilities [12]. Santra et al. also recommended PBE0 functional for predicting accurate H bond energies [47], while Neugebauer and coworkers concluded B3LYP „is reliable and far less computer-time-demanding method which gives sufficient accuracy with medium-sized basis sets“ [48]. Cybulski and Sadley used MP2/aug-cc-pVDZ level of theory to calculate vibrational Raman spectra of water dimer to water octamer [49], which can be compared with one of the first studies of Xantheas and Dunning [13].

First published matrix isolation studies using Raman spectroscopy were performed by Shirk and Claassen [50], Huber et al. [51], and Nibler and Coe [52]. The disadvantage of the Raman matrix isolation spectroscopy is higher concentration of the studied molecules with respect to the noble gas in order to detect the signal [53]. Hence it is no surprise that previous Raman work on water clusters has been done by different techniques: Wuelfert et al. reported coherent anti-Stokes Raman spectra of water dimers and higher clusters in seeded supersonic jets [54], while Otto et al. were the first to use slit jet expansion of water for detecting spontaneous Raman signal from water clusters [55]. The simple experimental setup that was used in our previous works on methanol [56], dimethylacetylene [57], acetylacetone [58], and

dioxolane [59] uses rather high molar ratio of water to argon (approx. 1:40) when compared to infrared matrix experiments which used up to 1:2000, and is perhaps best described as Raman spectroscopy of water in solid argon matrix. However, we hope it is a step towards future Raman matrix isolation spectroscopy experiments on water.

In the previous publication by our group, results of Raman study of water ice at low temperatures and pressure were presented, both for H₂O and D₂O [60]. Changes in slope of the temperature dependence of the $\nu(\text{OH})$ and $\nu(\text{OD})$ indicated that the phase transition ice XI \leftrightarrow I_h takes place at 84 K. The phase transition was found to be reversible. In the present article we discuss low temperature Raman spectra of H₂O and D₂O deposited in solid argon matrix at temperatures between 8 and 20 K, and solid amorphous water films that form upon heating the matrix to temperatures above 20 K. Molecular dynamics simulations using DLPOLY program served to model the relaxed water configurations in solid argon at 10 K. The resulting conformations of dimers, trimers, tetramers and pentamers were further optimized by Gaussian09 and their vibrational spectra calculated. These provided help in understanding the evolution of the spectral features. Our results are then compared to the recent publication of Vasylieva et al. [61] where vibrational spectra of water clusters in FCC argon are calculated using DFT/M06-2X method.

Experimental

Two series of experiments were performed, similar to ones described in ref [60]. The first setup is shown in Fig 1. Extra pure water was doubly distilled and then demineralized by SG Reinstwasser System RO 6 Sp to conductivity of 0.055 $\mu\text{S}/\text{cm}$. Fluka D₂O 99.8 % (D atom purity) was used as received. H₂O was repeatedly degassed using freeze-pump-thaw procedure and stored in a sample tube. Fixed volume of argon at atmospheric pressure was allowed to mix with water vapour in a tube linked to a gas valve. Sample tube of water was kept at room temperature, and the water vapour pressure calculated for $T = 295$ K estimated from [62] to be 2.61 kPa. On opening of the valve between sample tube and the cold finger of the CTI Cryogenics model 21 cryostat chamber, the argon and water vapour mixture (ratio of Ar to H₂O was 38.8) solidified on gold-plated surface which was cooled to 8 K or 10 K. DILOR Z24 a triple grating spectrometer equipped with a photon counting detection was used for spectra recording. The entrance slit was 300 μm and the spectral slitwidth 2 cm^{-1} .

The second experimental setup relating to H₂O only was essentially the same, only a new CCS 350 Janis Research closed cycle He cryostat with Lake Shore 331 temperature controller was used, and the same gold-plated surface was mounted inside the cooled chamber. Spectra were recorded with T64000 Horiba-JobinYvon Raman spectrometer, operating in triple subtractive mode. Raman spectra were recorded in multiwindow option, from 2800 to 3800 cm^{-1} . Green line at 514.5 nm of the Coherent INNOVA 400 laser served as an excitation source in both setups. The beam power used was 70 mW.

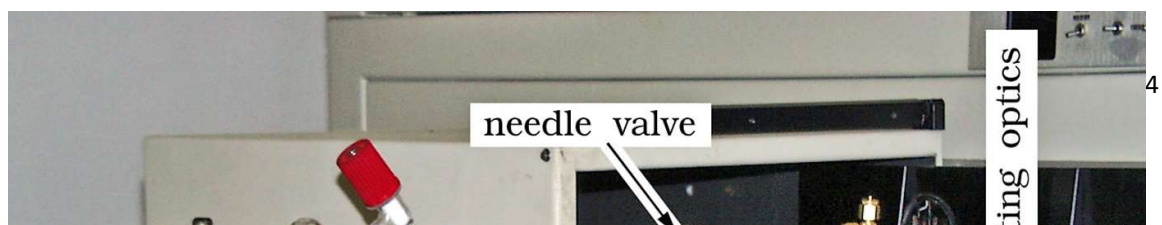


Fig. 1. Deposition of water in solid argon using closed cycle He cryostat and DILOR Z24 Raman spectrometer (setup I).

Computational details

Amorphous water

For calculating the vibrational density of states of an amorphous system, molecular dynamics is a method of choice. Here it was used for calculating vibrational density of states of pure amorphous water at 120 K in low frequency region and comparing it with a recorded low frequency Raman spectrum of water at the same temperature. For simulations we used DLPOLY software [63] and NMOLDYN program [64]. Briefly, velocity autocorrelation function (VACF) was calculated from velocities of oxygen and hydrogen atoms, sampled every 1 fs using nMOLDYN program [64]. On performing Fourier transformation of VACF (using nMOLDYN) theoretical vibrational density of states (VDOS) is obtained. Water molecule was assumed rigid, $r_{OH} = 0.9572 \text{ \AA}$, the HOH angle being 104.52° . TIP4P/Ice potential was used for description of intermolecular interaction [65]. Two charges equal to $0.52 e$ were distributed among atoms: two positive $+q$ at the positions of hydrogen atoms, and a third negative $-2q$ placed on a dummy-atom situated midway between hydrogens, on a bisecting line of HOH angle and 0.1577 \AA away from oxygen atom. The only other interaction besides Coulombic was Van der Waals interaction term between oxygen atoms. The system consisted of 2048 molecules and the side of simulation cube was 24.5058 \AA . The equilibration run was

performed in Hoover NPT ensemble which took 4 ps to equilibrate. The production run was performed in NVE ensemble, with the time-step 1 fs and total time 4 ps. The resulting low frequency vibrational density of states is displayed in Fig 2.

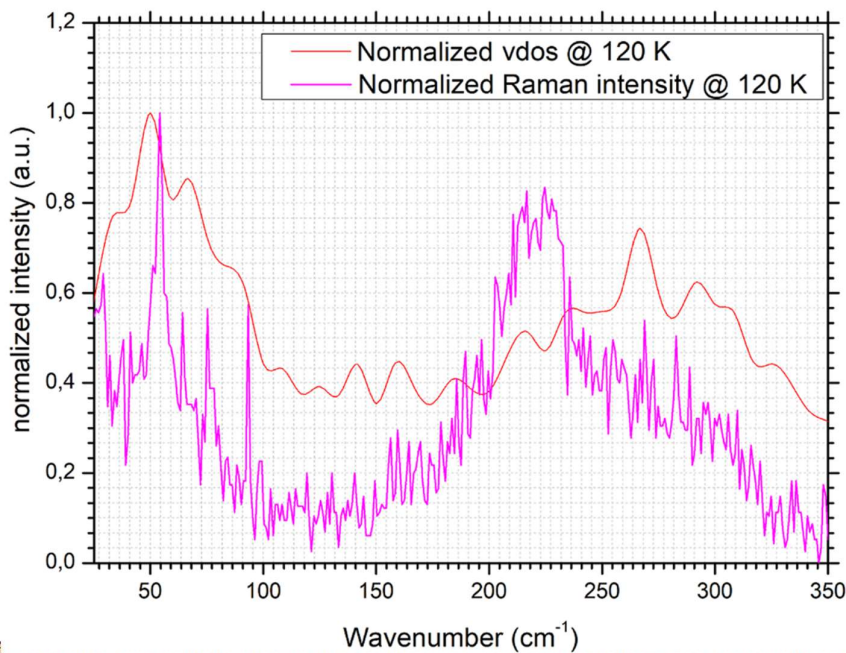


Figure 2. Comparison of experimental Raman intensity and calculated vibrational density of states of liquid water at 120 K and calculated vibrational density of states.

The agreement is qualitatively good, although the intensities of the band at 220 cm^{-1} and 270 cm^{-1} are reversed.

Water in argon matrix

Each starting configuration of water molecules embedded in argon matrix was created by inserting 13 water molecules into an FCC argon crystal lattice having lattice constant of 5.25 Å. The size of the simulation box was a cube with size of 26.25 Å which contained 500 argon atoms. Thus, one obtained a matrix ratio of 500:13 ($\approx 38:1$). Water molecules were modelled with SPC water model and Van der Waals interaction between water molecules and argon atoms [66]. In order that water molecules properly mix with argon and reorient as randomly as possible, the first molecular dynamics simulation run undertaken with DLPOLY 2.16 software was conducted under conditions of 300 K and zero pressure, in Berendsen NPT ensemble. Then the temperature was lowered to 10 K and the production run lasted for 40000 steps, one time-step being 1 fs (Supplementary Fig S1). Finally, from the output file the coordinates of water molecules forming multimers were extracted and then optimized by Gaussian09, using PBE1PBE (code name for PBE0 in Gaussian) and B3LYP functionals with aug-cc-pVDZ basis set (see Supplementary Table S1) [67]. We discuss further on conformers for which all calculated frequencies were positive; their geometries were the result of subsequent geometry optimization. As we were interested in assigning OH vibrations of water clusters, our primary goal was to list all OH stretching vibrations from highest to lowest for a reasonable number of multimers, and to compare them with the wavenumbers of the

observed bands. Theoretical values surpass the observed ones by far, therefore scaling theoretical values with the factor of 0.968 as done by Hirabayashi and Yamada [41] can be done for practical purpose of comparison with experiment. We used scaling factor of 0.9639, obtained by dividing the value of the observed symmetric stretching ν_1 determined by Avila for water vapour – 3660 cm^{-1} – with the value calculated for ν_1 using B3lyp/cc-aug-pVDZ level of theory for H_2O monomer: 3797 cm^{-1} . The calculated values of normal modes for O-H stretching motions for the 5 stable configurations of $(\text{H}_2\text{O})_n$, $n = 1-5$ and an open chain trimer are given in the Supplementary Table S1. The energies of multimers corrected with zero-point vibration energy are provided in the Supplementary Table S2, together with the calculated energies of hydrogen bonds in each multimer.

Results and Discussion

An overview of Raman spectra of H_2O and D_2O deposited in solid argon on gold plated surface at 10 K between 2000 and 2800 cm^{-1} (D_2O) or between 2800 and 3800 cm^{-1} (H_2O) is shown in Fig 3 (series I of experiments). Observed bands are qualitatively very much alike except that D_2O bands are shifted as expected and a $\nu(\text{N}_2)$ stretching band at 2330 cm^{-1} of trace N_2 is observed (Table 1). The bands observed at 3706, 3694, 3642, 3636 and 3576 cm^{-1} (Fig 3, series I) are observed at 3707, 3640, 3635 and 3575 cm^{-1} in the second series of experiments (Fig 4, spectrum at the bottom). When different needle valve aperture for deposition was used in series II, the spectrum at the top in Fig 4 was recorded: here the bands observed form different pattern. Instead of one band at 3707 cm^{-1} , there are four bands at 3726, 3714, 3698 and 3692 cm^{-1} . To bands at 3640 and 3635 cm^{-1} there correspond two bands at 3636 and 3631 cm^{-1} , while bands at 3575 and 3566 cm^{-1} have no counterparts (Fig 4). Instead, in place of weak 3475 cm^{-1} band there are broad bands at 3533, 3504 and 3452 cm^{-1} (Fig 4, at the top). Part of the explanation for this difference maybe stems out of the time duration of spectra acquisition. Series I of experiments was done using a sequentially scanning spectrometer with a photon counting detector, with time constant varying between 1 s and 4 s. Total acquisition time for the spectrum of H_2O shown in Fig 3 was 20 min. On the contrary, the spectra shown in Fig 4 were recorded with a multichannel detector having an array of 256×1024 pixels, and the whole spectral interval was recorded in tens of seconds. In other words, during the acquisition of spectrum from series I, much longer time has elapsed, and water molecules had time to aggregate into multimers (hence the occurrence of medium intensity broad bands at 3187, 3300 and 3419 cm^{-1} in spectrum shown in Fig 3). The two spectra shown in Fig 4 differ in the choice of valve aperture used for spraying water vapour/argon mixture onto the golden plate, the spectrum at the bottom of Fig 4 having many bands in common as the spectrum from Fig 3.

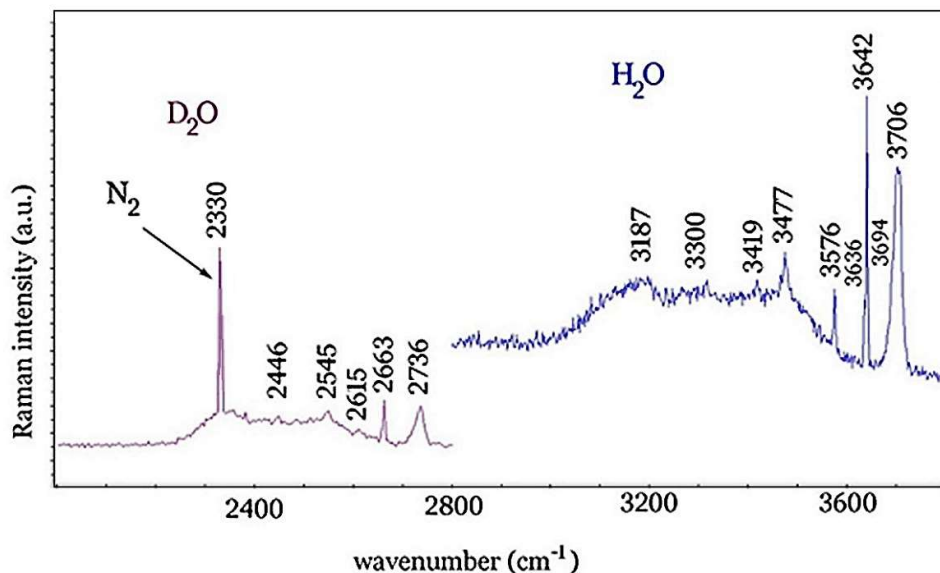


Figure 3. Raman spectra of the H₂O and D₂O in argon matrix at 10 K in the OH stretching and OD stretching region (series I of experiments). Small traces of nitrogen were present, as evidenced by the 2330 cm⁻¹ band in Raman spectrum of deposited D₂O. Bands are listed in Table 1. Raman spectrum of H₂O is shifted vertically for clarity.

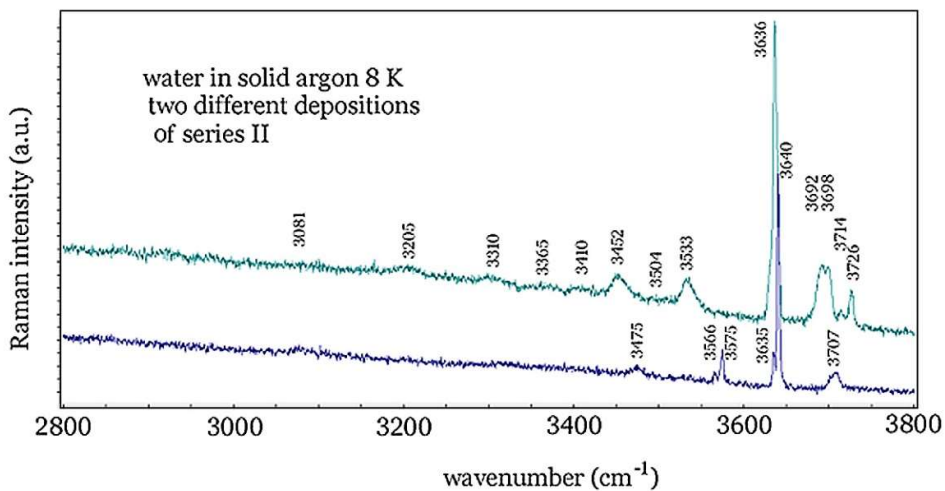


Figure 4. Raman spectrum of H₂O in solid argon matrix at 8K (series II of experiments, two different needle valve apertures). For bands assignment see Table 1.

We explain the assignment given in Table 1 by comparing the reported positions of Raman bands of water vapor [19] with bands observed in previous matrix isolation and jet expansion experiments [32-36, 55]. We discuss experimental data in relation to calculated vibrations by Vasylieva et al for water multimers embedded in argon matrix [61], as well as to our own predicted bands for free water clusters.

Fundamental transitions of free water molecule observed in Raman spectra of water vapour by Avila et al. include asymmetric OH stretching vibration ν_3 $|001\rangle_{J=0}$ Q branch at 3710 cm^{-1} with sub bands proceeding to lower wavenumbers and the ν_1 $|100\rangle_{J=0}$ Q branch starting below 3660 cm^{-1} [19]. Based on the strong intensity of the 3642 cm^{-1} (series I, Fig 3) and 3640 cm^{-1} band (series II, Fig 4), we assign them to the symmetric stretching vibration ν_1 of water monomer. The observed shift of approximately 20 cm^{-1} from the value in vapour [19] can be explained as a result of interaction with argon matrix. The results of Vasylieva et al. who calculated fundamental vibrations of water monomer and dimer when placed among argon atoms distributed on sites of face centered cubic lattice depend on the vacancy size of water molecule (whether it has been exchanged with two or one argon atom). Specifically, the symmetric stretching mode ν_1 of H_2O shifted to lower wavenumbers by 39.1 cm^{-1} , and the asymmetric stretching mode ν_3 shifted by 43.6 cm^{-1} if only one argon atom was removed from lattice in order to accommodate water. If two argon atoms were removed and one water molecule fitted in, ν_1 shifted only by 7.1 cm^{-1} and ν_3 shifted for 13.8 cm^{-1} towards lower wavenumbers (Table VIII in [61]).

Otto et al. recorded Raman spectra of jet cooled water clusters and reported ν_1 of water monomer at 3657 cm^{-1} , while the ν_1 of the acceptor molecule of $(\text{H}_2\text{O})_2$ was assigned to 3651 cm^{-1} band [55]. The strong band at 3706 cm^{-1} (Fig 3) and the weak band observed at 3707 cm^{-1} (Fig 4) are close to the position of 3710 cm^{-1} band to which Vasylieva et al. assigned the free OH stretching of the dimer donor molecule, while they predict the asymmetric stretching ν_3 of the dimer acceptor at 3715 cm^{-1} [61]. For all four fundamental OH stretching vibrations of the dimer, their calculated shifts in argon matrix are close to 25 cm^{-1} towards lower wavenumbers. Indeed, if one adds the shift of -25 cm^{-1} to values of fundamental vibrations assigned to water dimer in vapour phase by Huang and Miller [23, 24] – 3745.48 cm^{-1} ν_3 acceptor, 3730 cm^{-1} ν_3 donor, 3600 cm^{-1} ν_1 acceptor and 3530 cm^{-1} ν_1 donor – one would obtain expected positions of $(\text{H}_2\text{O})_2$ in the OH stretching region close to 3720 , 3705 , 3575 and 3505 cm^{-1} . Therefore, we assigned 3706 cm^{-1} (series I) and 3707 cm^{-1} (series II) to ν_3 vibration of donor molecule in the dimer, and the 3714 cm^{-1} band (series II, Fig 4) to the ν_3 of the dimer acceptor molecule. In this way, the band observed at the highest wavenumber (3726 cm^{-1}) is assigned to the antisymmetric stretching ν_3 of the water monomer (Fig 4).

Our calculations on free multimers predict that an open chain trimer has some normal modes very close to those of dimer (two vibrations at 3753 cm^{-1} compared to 3755 and 3734 cm^{-1} , scaled values; see Supplementary Table S1 and Fig 5). For the cyclic trimer scaled free OH stretching vibrations are predicted at 3731 , 3730 and 3726 cm^{-1} (calculated with B3LYP functional). In cyclic tetramer and pentamer the scaled free OH vibrations comprise one mode at 3725 cm^{-1} , two modes at 3724 cm^{-1} and one at 3723 cm^{-1} (tetramer), while for cyclic planar pentamer they are at 3730 , 3728 , 3727 , 3725 and 3724 cm^{-1} (scaled using 0.9639 as a scaling factor). Bearing in mind that we observe vibrations of water in argon matrix, we assign the 3692 cm^{-1} band to free OH vibration of the tetramer and pentamer, while the 3698 cm^{-1} band is assigned to the free OH vibration of the trimer. Bentwood et al. observed two bands

at 3700 and 3695 cm^{-1} [34], while Ayers and Pullin observed a band at 3693.8 cm^{-1} [33] (Table 1).

Due to hydrogen bonding, $\nu(\text{OH})$ of the donor OH groups are significantly shifted to lower wavenumbers. The medium band observed at 3576 cm^{-1} (series I, Fig 3) and 3575 cm^{-1} (series II, Fig 4) are assigned to dimer donor vibration. Continuing our discussion to the lower wavenumber part of the spectra, we assign the 3533 cm^{-1} medium weak band and 3504 cm^{-1} broad band to water trimer. Ceponkus et al. [40] attributed several bands in this region to the cyclic form of $(\text{H}_2\text{O})_3$: 3529.6 cm^{-1} , 3518 cm^{-1} (shoulder) and a very broad band at 3505 cm^{-1} . Engdahl and Nelander assigned the bands at 3516 cm^{-1} and 3702.2 cm^{-1} to water trimer, just as Bentwood et al. [34]. Although it has been agreed that the cyclic form of $(\text{H}_2\text{O})_3$ is the stable form of water trimer [38], in the calculated vibrational spectrum in the harmonic approximation modes are grouped roughly into two spectral intervals (Supplementary Table S1). Three modes corresponding to free OH groups are calculated at 3731, 3730 and 3726 cm^{-1} , and the other three at 3464, 3455, and 3394 cm^{-1} using B3LYP functional and the scaling factor of 0.9639. However, if PBE0 functional was applied (code name PBEPBE1 in Gaussian09), scaled values of fundamental vibrations include modes at 3487, 3477 and 3407 cm^{-1} (Supplementary Table S1). Therefore, the medium band at 3475 cm^{-1} (Fig 3, Fig 4) is assigned to cyclic trimer. Inspection of calculated scaled fundamentals in the OH stretching region shows no bands are predicted for cyclic trimer in the region of 3500 – 3700 cm^{-1} , but for open chain trimer the situation is different. At the B3LYP/aug-cc-pVDZ level of theory, one finds for open chain trimer two modes at 3753 cm^{-1} , one at 3654, 3651, 3634 and 3551 cm^{-1} (Supplementary Table S1). The lowest one at 3551 cm^{-1} lies 13 cm^{-1} above the 3533 cm^{-1} band observed in series II (Fig 4, spectrum at the top). The overview of calculated Raman spectra for $(\text{H}_2\text{O})_n$, $n=1,2,3,4,5$ is given on the right of Fig 5.

Turning to $(\text{H}_2\text{O})_4$ and $(\text{H}_2\text{O})_5$ multimers, there is also characteristic grouping of calculated wavenumbers for OH stretching modes above 3700 cm^{-1} into those involving free OH groups, and those that are bound: for cyclic tetramer four normal modes of the bound OH groups are expected at 3344, 3311, 3301 and 3209 cm^{-1} , while for cyclic planar pentamer they fall between 3363 and 3152 cm^{-1} (Supplementary table S1). The OH stretching mode lying at the lowest wavenumber is predicted to have highest Raman intensity (Fig 5, right), and this is valid for $(\text{H}_2\text{O})_n$, $n=2-5$. This strongest Raman band shifts to lower wavenumbers as the number of water molecules in cluster rises (Fig 5) and could explain the rise of intensity in Raman bands as the matrix is heated above the temperature of argon evaporation (Fig 5, left). Above 28 K only water is adsorbed on golden plate and strong broad bands overlap between 3100 and 3400 cm^{-1} . At the same time, all OH stretching modes of the free OH groups merge and overlap into a single band at 3689 cm^{-1} (18 K) or at 3678 cm^{-1} (34 K). This has been noticed in previous studies of amorphous confined water [68,69].

Our assignation of trimer bands correlates 3533 cm^{-1} and 3504 cm^{-1} bands with OH stretching vibrations of the bound hydroxyl groups (Fig 4), the band at 3310 cm^{-1} was assigned to tetramer, and the band at 3205 cm^{-1} to water pentamer. Hirabayashi and Yamada - who applied the scaling factor of 0.968 - presented assignments which include book and cage hexamer bands in the interval between 3420 and 3480 cm^{-1} , that is between $(\text{H}_2\text{O})_3$ and $(\text{H}_2\text{O})_4$ bands [41]. They distinguished cyclic hexamer from other $(\text{H}_2\text{O})_6$ multimers by assigning the 3360 cm^{-1} band to the cyclic form, and the 3224 cm^{-1} band to another form. We assign therefore the 3365 cm^{-1} band to cyclic hexamer.

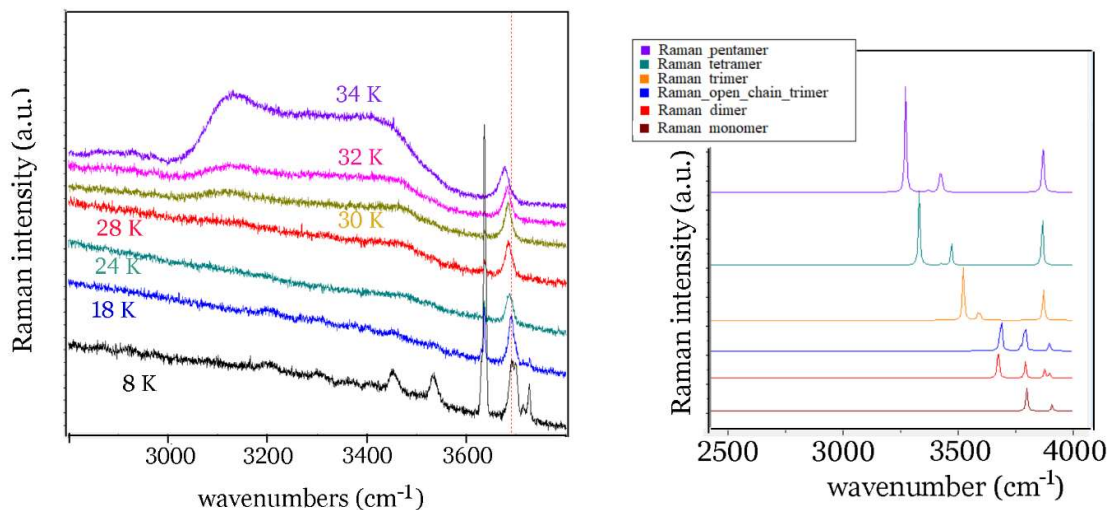


Figure 5. Left: Temperature dependence of Raman spectra of water H₂O recorded at 8 K, 18 K, 24 K, 28 K, 30 K, 32 K and 34 K. At 28 K and above argon matrix melts and water is adsorbed on gold plated surface. Right: Theoretical Raman spectra of water multimers from top down: cyclic planar pentamer, cyclic planar tetramer, cyclic trimer, open chain trimer, dimer and monomer (unscaled) obtained with B3LYP functional.

Conclusion

To summarize, Raman spectra of water in solid argon at temperatures as low as 8 K enable us to follow water aggregation from monomer to dimer, trimer and other multimer species up to hexamer. At temperatures equal to 24 K and higher argon evaporates and water agglomerates into bulk amorphous water. This work is the first one to report Raman spectra of water in solid argon matrix.

Acknowledgement

This work was supported by Centre for Advanced Materials and Sensing Devices, project number EK-EFRR-KK.01.1.1.01.0001.

References

1. Chun-Jen Huang, Ying-Chih Chang: Construction of Cell–Extracellular Matrix Microenvironments by Conjugating ECM Proteins on Supported Lipid Bilayers, *Front. Mat.* **6** (2019) art. no. 39. <https://www.frontiersin.org/articles/10.3389/fmats.2019.00039/full>

2. N. Taricska, M. Bokor, D. K. Menyhárd, K. Tompa, A. Perczel: Hydration shell differentiates folded and disordered states of a Trp-cage miniprotein, allowing characterization of structural heterogeneity by wide-line NMR measurements, *Scientific Reports* **9** (2019) art. no 2947. <https://www.nature.com/articles/s41598-019-39121-5>
3. K. Rezaei, E. Jenab, F. Temelli: Effects of Water on Enzyme Performance with an Emphasis on the Reactions in Supercritical Fluids, *Crit. Rev. Biotechnol.* **27** (4) (2007) 183-195. <https://www.tandfonline.com/doi/full/10.1080/07388550701775901>
4. Chao-Jun Li, B. M. Trost: Green chemistry for chemical synthesis, *PNAS* **105** (2008) 13197 - 13202. <https://www.pnas.org/content/105/36/13197>
5. M. Kinoshita, T. Hayashi: Accurate and rapid calculation of hydration free energy and its physical implication for biomolecular functions, *Biophys. Rev.* **12** (2020) 469-480. <https://www.ncbi.nlm.nih.gov/pmc/articles/PMC7242554/>
6. Wikimedia Commons: The Phase Diagram of Water
[https://commons.wikimedia.org/wiki/File:Phase diagram of water.svg](https://commons.wikimedia.org/wiki/File:Phase_diagram_of_water.svg)
7. L. Pauling: The Structure and Entropy of Ice and of Other Crystals with Some Randomness of Atomic Arrangement, *J. Am. Chem. Soc.* **57** (1935) 2680 -2684. <https://pubs.acs.org/doi/abs/10.1021/ja01315a102>
8. J. Teixeira: The physics of liquid water, *J. Phys. IV France* **03** (1993) C1-163-C1-169. <https://jp4.journaldephysique.org/articles/jp4/abs/1993/01/jp4199303C114/jp4199303C114.html>
9. F. N. Keutsch, R. J. Saykally: Water clusters: Untangling the mysteries of the liquid, one molecule at a time, *PNAS* **98** (2001) 10533 – 10540. <https://www.pnas.org/content/98/19/10533>
10. J. M. Headrick, E. G. Diken, R. S. Walters, N. I. Hammer, R. A. Christie, Jun Cui, E. M. Myshakin, M. A. Duncan, M. A. Johnson and K. D. Jordan: Spectral signatures of hydrated proton vibrations in water clusters, *Science* **308** (2005) 1765 – 1769. <https://pubmed.ncbi.nlm.nih.gov/15961665/>
11. J. P. Heindel, Qi Yu, J. M. Bowman, S. S. Xantheas: Benchmark Electronic Structure Calculations for $\text{H}_3\text{O}^+(\text{H}_2\text{O})_n$, $n=0-5$, Clusters and Tests of an Existing 1,2,3-Body Potential Energy Surface with a New 4-Body Correction, *J. Chem. Theory Comput.* **14** (2018) 4553 – 4566. <https://pubmed.ncbi.nlm.nih.gov/30103598/>
12. J. R. Hammond, N. Govind, K. Kowalski, J. Autschbach, S. S. Xantheas: Accurate dipole polarizabilities for water clusters $n=2-12$ at the coupled-cluster level of theory and benchmarking of various density functionals, *J. Chem. Phys.* **131** (2009) art. no. 214103, 9 pages. <https://aip.scitation.org/doi/10.1063/1.3263604>
13. S. S. Xantheas, T. H. Dunning Jr.: *Ab initio* studies of cyclic water clusters $(\text{H}_2\text{O})_n$, $n=1-6$. I. Optimal structures and vibrational spectra, *J. Chem. Phys.* **99** (1993) 8774 – 8792. <https://aip.scitation.org/doi/10.1063/1.465599>

14. M. F. Chaplin: Structure and Properties of Water in its Various States, Encyclopedia of Water: Science, Technology, and Society, Wiley Online Library, <https://doi.org/10.1002/9781119300762.wsts0002> , accessed 05.11.2021.
15. G. Bonner: The vibrational spectrum of water vapour, Phys. Rev. **46** (1934) 458 – 464. <https://authors.library.caltech.edu/4829/1/BONpr34a.pdf>
16. J. Tennyson, P.F. Bernath, L. R. Brown, A. Campargue, A. G. Császár, L. Daumont et al.: A database of water transitions from experiment and theory (IUPAC Technical Report), Pure Appl. Chem. **86** (2014) 71 – 83. https://digitalcommons.odu.edu/cgi/viewcontent.cgi?article=1112&context=chemistry_fac_pubs
17. G. Avila, G. Tejada, J. M. Fernández, S. Montero: The rotational Raman spectra and cross sections of H₂O, D₂O, and HDO, J. Mol. Spectrosc. **220** (2003) 259 – 275. https://www.researchgate.net/publication/244400429_The_rotational_Raman_spectra_and_cross_sections_of_H_2O_D_2O_and_HDO
18. L. S. Rothman, I. E. Gordon, A. Barbe, D. C. Benner, P. F. Bernath et al.: The HITRAN 2008 molecular spectroscopic database, J. Quant. Spectrosc. Radiat. Transfer **110** (2009) 533 - 572. <https://lweb.cfa.harvard.edu/atmosphere/publications/HITRAN2008.pdf>
19. G. Avila, J. M. Fernandez, G. Tejada, S. Montero: The Raman spectra and cross-sections of H₂O, D₂O, and HDO in the OH/OD stretching regions, J. Mol. Spectrosc. **228** (2004) 38-65. <https://www.sciencedirect.com/science/article/abs/pii/S0022285204001961>
20. T. R. Dyke, J. S. Muentzer: Molecular beam electric deflection studies of water polymers, J. Chem. Phys. **57** (1972) 5011 – 5012. <https://aip.scitation.org/doi/abs/10.1063/1.1678174?journalCode=jcp>
21. T. R. Dyke, K. M. Mack, J. S. Muentzer: The structure of water dimer from molecular beam electric resonance spectroscopy, J. Chem. Phys. **66** (1977) 498 – 510. <https://aip.scitation.org/doi/10.1063/1.433969>
22. N. Pugliano, R. J. Saykally: Measurement of Quantum Tunneling Between Chiral Isomers of the Cyclic Water Trimer, Science **257** (1992) 1937–1940. <https://www.science.org/doi/abs/10.1126/science.1411509>
23. Z. S. Huang, R. E. Miller: High-resolution near-infrared spectroscopy of water dimer, J. Chem. Phys. **91** (1989) 6613-6631. <https://aip.scitation.org/doi/abs/10.1063/1.457380>
24. Z. S. Huang, R. E. Miller: Sub-Doppler resolution infrared spectroscopy of water dimer, J. Chem. Phys. **88** (1988) 8008-8009. <https://aip.scitation.org/doi/abs/10.1063/1.454258?journalCode=jcp>
25. M. F. Vernon, D. J. Krajnovich, H. S. Kwok, J. M. Lisy, Y. R. Shen, Y. T. Lee: Infrared vibrational predissociation spectroscopy of water clusters by the crossed laser-molecular beam technique, J. Chem. Phys. **77** (1982) 47 – 57. <https://aip.scitation.org/doi/10.1063/1.443631>

26. R. H. Page, J. G. Frey, Y.-R. Shen, Y. T. Lee: Infrared predissociation spectra of water dimer in a supersonic molecular beam, *Chem. Phys. Lett.* **106** (1984) 373 – 376.
[https://doi.org/10.1016/0009-2614\(84\)85320-8](https://doi.org/10.1016/0009-2614(84)85320-8)
27. J. B. Paul, R. A. Provencal, C. Chappo, A. Petterson, R. J. Saykally: Infrared cavity ringdown spectroscopy of water clusters: O–D stretching bands, *J. Chem. Phys.* **109** (1998) 10201 – 10206. <https://aip.scitation.org/doi/10.1063/1.477714>
28. F. Huisken, M. Kaloudis, A. Kulcke: Infrared spectroscopy of small size-selected water clusters, *J. Chem. Phys.* **104** (1996) 17-25.
<https://aip.scitation.org/doi/10.1063/1.470871>
29. M. Van Thiel, E. D. Becker, G. C. Pimentel: Infrared Studies of Hydrogen Bonding of Water by the Matrix Isolation Technique, *J. Chem. Phys.* **27** (1957) 486 – 490.
<https://aip.scitation.org/doi/10.1063/1.1743753>
30. J. A. Glasel: Near-Infrared Absorption Spectra of Ortho- and Para-H₂O in Solid Xenon and Argon, *J. Chem. Phys.* **33** (1960) 252 – 255.
<https://aip.scitation.org/doi/abs/10.1063/1.1731093>
31. D. Forney, M. E. Jacox, W. E. Thompson: The Mid- and Near-Infrared Spectra of Water and Water Dimer Isolated in Solid Neon, *J. Mol. Spectrosc.* **157** (1993) 479 – 493.
<https://www.sciencedirect.com/science/article/abs/pii/S0022285283710374>
32. A. J. Tursi, E. R. Nixon: Matrix-Isolation Study of the Water Dimer in Solid Nitrogen, *J. Chem. Phys.* **52** (1970) 1521 – 1528. <https://aip.scitation.org/doi/abs/10.1063/1.1673163>
33. G. P. Ayers, A. D. E. Pullin: The i.r. spectra of matrix isolated water species—I. Assignment of bands to (H₂O)₂, (D₂O)₂ and HDO dimer species in argon matrices, *Spectrochim. Acta* **32A** (1976) 1629 – 1639.
<https://www.sciencedirect.com/science/article/abs/pii/0584853976802656>
34. R. M. Bentwood, A. J. Barnes, W. J. Orville-Thomas: Studies of Intermolecular Interactions by Matrix Isolation Vibrational Spectroscopy: Self-association of Water, *J. Mol. Spectrosc.* **84** (1980) 391 – 404.
<https://www.sciencedirect.com/science/article/abs/pii/0022285280900314>
35. J. P. Perchard: Anharmonicity and hydrogen bonding. III. Analysis of the near infrared spectrum of water trapped in argon matrix, *Chem. Phys.* **273** (2001) 217 – 233.
<https://www.sciencedirect.com/science/article/abs/pii/S0301010401004967>
36. S. Coussan, P. Roubin, J. P. Perchard: Infrared induced isomerizations of water polymers trapped in nitrogen matrix, *Chem. Phys.* **324** (2006) 527 – 540.
<https://www.sciencedirect.com/science/article/abs/pii/S0301010405006075>
37. J. Ceponkus, P. Uvdal, B. Nelander: On the structure of the matrix isolated water trimer, *J. Chem. Phys.* **134** (2011) art. no. 064309, 12 pages.
<https://aip.scitation.org/doi/10.1063/1.3551622>
38. F. N. Keutsch, J. D. Cruzan, R. J. Saykally: The water trimer, *Chem. Rev.* **103** (2003) 2533–2577.

http://www.cchem.berkeley.edu/rjsgrp/publications/papers/2003/278_keutsch_2003.pdf

39. A. Engdahl, B. Nelander: On the structure of the water trimer. A matrix isolation study, *J. Chem. Phys.* **86** (1987) 4831-4837. <https://aip.scitation.org/doi/abs/10.1063/1.452676>
40. J. Ceponkus, P. Uvdal, B. Nelander: Water Tetramer, Pentamer, and Hexamer in Inert Matrices, *J. Phys. Chem A* **116** (2012) 4842-4850. <https://pubs.acs.org/doi/abs/10.1021/jp301521b>
41. S. Hirabayashi, K. M. T. Yamada, Infrared spectra and structure of water clusters trapped in argon and krypton matrices, *J. Mol. Struct.* **795** (2006) 78 – 83. <https://www.sciencedirect.com/science/article/abs/pii/S0022286006001669>
42. S. Yoo, S. S. Xantheas „Structures, Energetics and Spectroscopic Fingerprints of Water Clusters $n=2-24$ “, Chapter 26 in: *Handbook of Computational Chemistry*, Ed. by J. Leczczyński et al., Springer International Publishing Switzerland 2017, pp. 1139-1173. <https://www.osti.gov/biblio/1364012-structures-energetics-spectroscopic-fingerprints-water-clusters>
43. V. A. Benderski, D. E. Makarov, C. A. Wight „Vibration-rotation tunneling spectroscopy of molecules and dimers“, Chapter 8 in *Advance in Chemical Physics Vol 88*, J. Wiley & Sons 1994, pp.261-307. <https://onlinelibrary.wiley.com/doi/10.1002/9780470141472.ch8>
44. S. S. Xantheas: Cooperativity and hydrogen bonding network in water clusters, *Chem. Phys.* **258** (2000) 225-231. <https://www.sciencedirect.com/science/article/abs/pii/S0301010400001890>
45. M. B. Day, K. N. Kirschner, G. C. Shields: Global Search for Minimum Energy $(\text{H}_2\text{O})_n$ Clusters, $n=3-5$, *J. Phys. Chem. A* **109** (2005) 6773-6778. <https://pubs.acs.org/doi/10.1021/jp0513317>
46. O. M6, M. Yañez, J. Elguero: Cooperative (nonpairwise) effects in water trimers: An *ab initio* molecular orbital study, *J. Chem. Phys.* **97** (1992) 6628 – 6638. <https://aip.scitation.org/doi/10.1063/1.463666>
47. B. Santra, A. Michaelides, M. Scheffler: On the accuracy of density-functional theory exchange-correlation functionals for H bonds in small water clusters: Benchmarks approaching the complete basis set limit, *J. Chem. Phys.* **127** (2007) art. no 184104, 9 pages <https://aip.scitation.org/doi/abs/10.1063/1.2790009>
48. J. Neugebauer, M. Reiher, B. A. Hess: Coupled-cluster Raman intensities: Assessment and comparison with multiconfiguration and density functional methods, *J. Chem. Phys.* **117** (2002) 8623-8633. <https://aip.scitation.org/doi/abs/10.1063/1.1506919>
49. H. Cybulski, J. Sadley: On the calculations of the vibrational Raman spectra of small water clusters, *Chem. Phys.* **342** (2007) 163-172. <https://www.sciencedirect.com/science/article/abs/pii/S0301010407004466>
50. J. S. Shirk, H. H. Claassen: Raman Spectra of Matrix-Isolated Molecules, *J. Chem. Phys.* **54** (1971) 3237. <https://aip.scitation.org/doi/abs/10.1063/1.1675322?journalCode=jcp>

51. H. Huber, G. A. Ozin, A. Vander Voet: The matrix Raman spectrum of monomeric tin dichloride in solid argon and nitrogen, *J. Mol. Spectrosc.* **40** (1971) 421 - 423.
<https://www.sciencedirect.com/science/article/abs/pii/0022285271901676?via%3Dihub>
52. J. W. Nibler, D. A. Coe: Depolarization Measurements in Raman Matrix Isolation Spectroscopy, *J. Chem. Phys.* **55** (1971) 5133.
<https://aip.scitation.org/doi/abs/10.1063/1.1675637?journalCode=jcp>
53. A. Kornath: Multi-channel Raman Matrix Isolation Spectroscopy, *J. Raman Spectrosc.* **28** (1997) 9 -14. [https://doi.org/10.1002/\(SICI\)1097-4555\(199701\)28:1<9::AID-JRS55>3.0.CO;2-7](https://doi.org/10.1002/(SICI)1097-4555(199701)28:1<9::AID-JRS55>3.0.CO;2-7)
54. S. Wuelfert, D. Herren, S. Leutwyler: Supersonic jet CARS spectra of small water clusters, *J. Chem. Phys.* **86** (1987) 3751 – 3753.
<https://aip.scitation.org/doi/abs/10.1063/1.451977?journalCode=jcp>
55. K. E. Otto, Zhifeng Xue, P. Zielke, M. A. Suhm: The Raman spectrum of isolated water clusters, *Phys. Chem. Chem. Phys.* **16** (2014) 9849 – 9858.
<https://pubs.rsc.org/en/content/articlelanding/2014/cp/c3cp54272f>
56. K. Furić, V. Mohaček, M. Mamić: Methanol in matrix isolated, vapour and liquid phase: Raman spectroscopic study, *Spectrochim. Acta A Molecular and Biomolecular Spectroscopy* **49** (1993) 2081 – 2087.
<https://www.sciencedirect.com/science/article/abs/pii/S0584853909910170>
57. V. Mohaček-Grošev, K. Furić: Low temperature Raman study of dimethylacetylene, *J. Mol. Struct.* **482-483** (1999) 653 – 659.
<https://www.sciencedirect.com/science/article/abs/pii/S002228609900023X>
58. V. Mohaček-Grošev, K. Furić, H. Ivanković: Luminescence and Raman spectra of acetylacetone at low temperatures, *J. Phys. Chem. A* **111** (2007) 5820 - 5827.
<https://pubs.acs.org/doi/10.1021/jp067157i>
59. V. Mohaček-Grošev, K. Furić, H. Ivanković: Observed bands in Raman and infrared spectra of 1,3-dioxolane and their assignments, *Vibrational Spectroscopy* **64** (2013) 101-107. <https://www.sciencedirect.com/science/article/abs/pii/S0924203112002056>
60. K. Furić, V. Volovšek: Water ice at low temperatures and pressures: New Raman results, *J. Mol. Struct.* **976** (2010) 174 – 180.
<https://www.sciencedirect.com/science/article/abs/pii/S0022286010002504>
61. A. Vasylieva, I. Doroshenko, S. Stepanian, L. Adamowicz: The influence of low-temperature argon matrix on embedded water clusters. A DFT theoretical study, *Low Temp. Phys.* **47** (2021) 242 – 249.
<https://aip.scitation.org/doi/abs/10.1063/10.0003525>
62. Vapor pressure of water calculator,
<http://www.endmemo.com/chem/vaporpressurewater.php>

63. W. Smith, T. R. Forrester: DL_POLY_2.0: A general-purpose parallel molecular dynamics simulation package, *J. Mol. Graphics* **14** (1996) 136 – 141.
<https://www.sciencedirect.com/science/article/abs/pii/S0263785596000434>
64. T. Róg, K. Murzyn, K. Hinsen, G. R. Kneller: nMoldyn: a program package for a neutron scattering oriented analysis of molecular dynamics simulations, *J. Comput. Chem.* **24** (2003) 657 – 667. <https://europemc.org/article/MED/12632481>
65. J. L. Abascal, E. Sanz, R. García Fernández, C. Vega: A potential model for the study of ices and amorphous water: TIP4P/Ice, *J. Chem. Phys.* **122** (2005) 234511.
<https://aip.scitation.org/doi/10.1063/1.1931662>
66. C. McBride: SklogWiki - Water models: SPC model of water
http://www.sklogwiki.org/SklogWiki/index.php/SPC_model_of_water
67. Gaussian 09, Revision A.02, M. J. Frisch, G. W. Trucks, H. B. Schlegel, G. E. Scuseria, M. A. Robb, J. R. Cheeseman, G. Scalmani, V. Barone, G. A. Petersson, H. Nakatsuji, X. Li, M. Caricato, A. Marenich, J. Bloino, B. G. Janesko, R. Gomperts, B. Mennucci, H. P. Hratchian, J. V. Ortiz, A. F. Izmaylov, J. L. Sonnenberg, D. Williams-Young, F. Ding, F. Lipparini, F. Egidi, J. Goings, B. Peng, A. Petrone, T. Henderson, D. Ranasinghe, V. G. Zakrzewski, J. Gao, N. Rega, G. Zheng, W. Liang, M. Hada, M. Ehara, K. Toyota, R. Fukuda, J. Hasegawa, M. Ishida, T. Nakajima, Y. Honda, O. Kitao, H. Nakai, T. Vreven, K. Throssell, J. A. Montgomery, Jr., J. E. Peralta, F. Ogliaro, M. Bearpark, J. J. Heyd, E. Brothers, K. N. Kudin, V. N. Staroverov, T. Keith, R. Kobayashi, J. Normand, K. Raghavachari, A. Rendell, J. C. Burant, S. S. Iyengar, J. Tomasi, M. Cossi, J. M. Millam, M. Klene, C. Adamo, R. Cammi, J. W. Ochterski, R. L. Martin, K. Morokuma, O. Farkas, J. B. Foresman, and D. J. Fox, Gaussian, Inc., Wallingford CT, 2016.
68. K. Kristinaityte, L. Dagys, J. Kausteklis, V. Klimavicius, I. Doroshenko, V. Pogorelov, N. R. Valvičiene, V. Balevicius: NMR and FTIR studies of clustering of water molecules: From low-temperature matrices to nano-structured materials used in innovative medicine, *J. Mol. Liq.* **235** (2017) 1-6.
<https://www.sciencedirect.com/science/article/abs/pii/S0167732216326174>
69. M. Erko, G. H. Findenegg, N. Cada, A. G. Michette, O. Paris: Confinement-induced structural changes of water studied by Raman scattering, *Phys. Rev. B* **84** (2011) art.no. 104205, 8 pages. <https://journals.aps.org/prb/abstract/10.1103/PhysRevB.84.104205>

Table 1. Observed OH and OD stretching bands of water molecules in solid argon matrix at 8 K (this work) compared with data from literature (cm⁻¹).

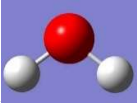
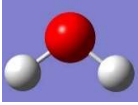
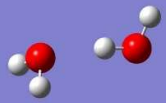
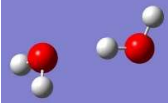
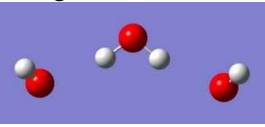
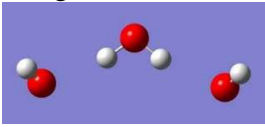
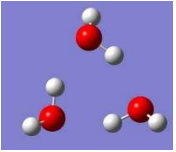
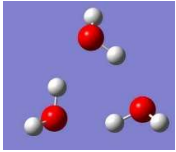
	Raman This work Series I (Fig 3)	Raman This work Series II (Fig 4)		Assignment	Raman Otto et al. [55]	IR Coussan et al. 2006. [36]	IR / Ar Perchard 2001. Nonrot.species only [35]	IR / Ar Bentwood et al. 1980. [34]	IR Ayers & Pullin 1976. [33]	IR Tursi et al. 1970. [32]
H ₂ O	3706 s,br 3694 m,sh 3642 s 3636 m,sh 3576 m	3726 mw 3714 w 3698 m 3692 m 3636 s 3631 m,sh	3707 w 3640 s 3635 w 3575 mw 3566 w	v ₃ monomer v ₃ dimer acceptor v ₃ dimer donor free OH Tri free OH Tet, Pent v ₁ monomer v ₁ dimer acceptor v ₁ dimer donor	3730 D free OH 3721 3711 mult.freeOH 3657 M 3651 DA 3606 D (OH) _b 3602 D (OH) _b	3727.5 3715.7 3699.8 3634.9 3627.9 3550.4	3737.8 v ₃ DA 3736 v ₃ M 3715.7 v ₃ DA 3708.0 v ₃ DD 3638.3 M 3633.1 v ₁ DA 3574.0 v ₁ DD	3733 3726 3709 3700, 3695 3638 3634 3612 3574 3566, 3565	3736 w 3722 w 3709.5 m 3702.5 w 3693.8 vw 3639.3 w 3634.1 w 3624.2 vw 3574.5 vs 3568 w	3740 vw 3725.7 s 3714.4 m 3697.7 m 3688 m 3632.5 m 3625.6 w 3547.5 m
	3477 m 3419 mw, vbr 3300 mw,vbr 3187 mw, vbr	3533 mw,br 3504 vw 3452 mw 3410 vw 3365 vw 3310 vw 3205 vw	3475 w	trimer donor trimer donor cyclic trimer cyclic trimer cyclic trimer cyclic hexamer tetramer (OH) _b pentamer (OH) _b	3548 Tri (OH) _b 3533 Tri(OH) _b 3506 M (OH) _b 3491 Tri (OH) _b 3438 Tet (OH) _b 3401 Tet (OH) _b 3355 P (OH) _b 3347 Tet (OH) _b 3334 Tet (OH) _b 3310 P (OH) _b 3214 trimer	3528 m 3515 s 3472 w,br 3444 w,br 3414 w 3390.4 m 3372.3 s 3336 w,br 3325 m,br 3280 m,br 3212 w,br 3184 w	3528 sh 3516 3418 sh 3409 sh 3391 sh 3372 3332 3325 3230 3205 3182.3 2v ₂ DD 3150.8 2v ₂ DA 3141.2 2v ₂ M	3540 mult. 3528, 3516 3500 3445 3415 3390 3374 3327 3320 3212 3150	3525 m 3390 mw 3372 mw 3329 w 3209 vw	3510 w 3435 vw 3355 m 3320 w 3220 w

Table 1. continued

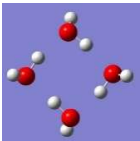
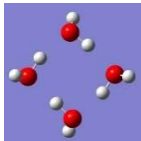
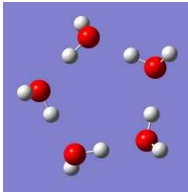
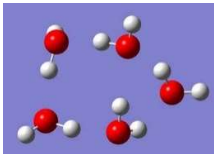
	Raman This work Series I (Fig 3)	Assignment	Raman Otto et al. 2014. [55]	Raman Otto et al. 2014. [55]	IR Coussan et al. 2006. [36]	IR Bentwood et al. 1980. [34]	IR Ayers & Pullin 1976. [33]	IR Tursi et al. 1970. [32]
D ₂ O	2736 m, br	v ₃ monomer	2762 dimer free OH 2756 trimer free OH 2748 Tet, P	2762 2756 2748	2765.9 2757.5 2738.6	2772 2766 2746 2738, 2733	2769.5 vw 2765.9 w 2754.7 2746.4 s 2738, 2733 m	2785 vw 2764.6 s 2756.6 m 2737.6 m 2724 m
	2663 m	v ₁ monomer	2672 monomer 2654 dimer acceptor	2672 2654	2655.4 2650.3	2658 2655	2658.5 w 2654.8 w	2655 m 2650 w 2618.9 vw 2616.6 vw
	2615 mw	v ₁ dimer donor	2637 dimer OH bound 2633 dimer OH bound 2591 Tri	2637 2633		2615 2600, 2592	2614.8 vs	
	2545 m,br	trimer	2566 multimer 2562 2559 Tri OH bound 2477 P 2465 Tet 2459 Tet 2443 P 2375 bending overtone	2591 2566, 2562 2559	2599.6 2578.8 2545 br 2487.5 s	2580 2496 2488 2456	2599.5 vw 2591.5 vw 2579.5 s 2496 w 2488 ms 2456 m	2599.1 m 2575 w 2475 m 2450 w 2380 vw
	2446 mw, br	tetramer (OH) _b						
	2350 mw,br	pentamer (OH) _b						

M- monomer, D- dimer, Tri- trimer, Tet- tetramer, P- pentamer, w- weak, m- medium, s- strong, br- broad, v- very, DA- dimer acceptor, DD- dimer donor, mult.- multimer

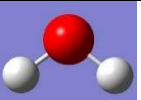
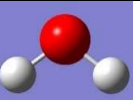
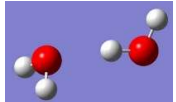
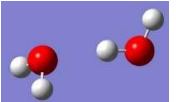
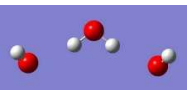
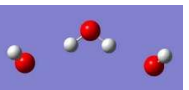

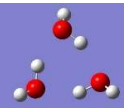
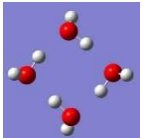


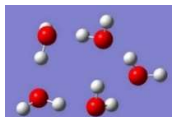
Supplementary Table S1. Unscaled and scaled calculated values of OH stretching vibrations of (H₂O)_n stable configurations for *n* = 1-5 including open chain trimer using B3LYP and PBE0 density functionals with the same aug-cc-pVDZ basis set (cm⁻¹). Scaling factor is 0.9639.

(H ₂ O) _n	B3LYP		(H ₂ O) _n	PBE0	
	unscaled	scaled		unscaled	scaled
<i>n</i> = 1 	3906 3797	3781 3660	<i>n</i> = 1 	3917 3799	3776 3662
<i>n</i> = 2 	3896 3874 3790 3672	3755 3734 3653 3539	<i>n</i> = 2 	3955 3934 3847 3714	3812 3792 3708 3580
<i>n</i> = 3 	3894 3894 3791 3788 3770 3684	3753 3753 3654 3651 3634 3551	<i>n</i> = 3 	3913 3913 3805 3802 3784 3693	3772 3772 3668 3665 3647 3560
<i>n</i> = 3 	3871 3870 3866 3594 3584 3521	3731 3730 3726 3464 3455 3394	<i>n</i> = 3 	3928 3926 3922 3618 3607 3535	3786 3784 3780 3487 3477 3407

Supplementary Table S1. Continued

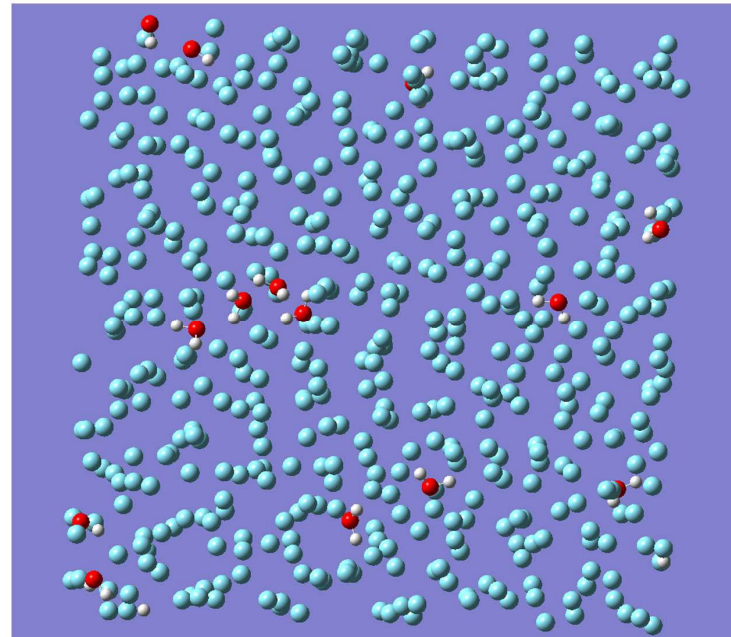
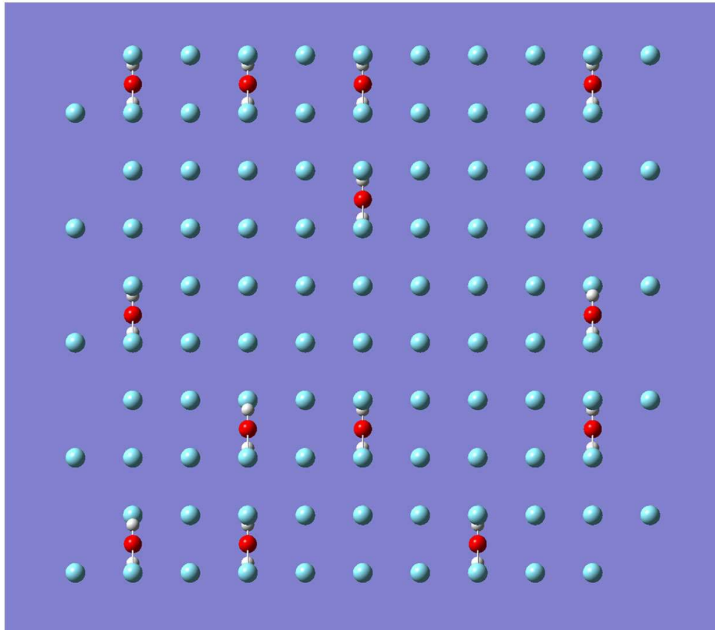
<p>$n = 4$</p> 	<p>3865 3864 3863 3862 3469 3435 3425 3329</p>	<p>3725 3724 3724 3723 3344 3311 3301 3209</p>	<p>$n = 4$</p> 	<p>3953 3932 3919 3917 3498 3453 3405 3313</p>	<p>3810 3790 3778 3776 3372 3328 3282 3193</p>
<p>$n = 5$ planar</p> 	<p>3870 3868 3867 3865 3863 3427 3418 3370 3362 3270</p>	<p>3730 3728 3727 3725 3724 3303 3295 3248 3241 3152</p>	<p>$n = 5$ nonplanar</p> 	<p>3929 3927 3925 3916 3776 3690 3624 3411 3356 3266</p>	<p>3787 3785 3783 3775 3640 3557 3493 3288 3235 3148</p>

Supplementary Table S2. Calculated values E_{tot} of stable $(\text{H}_2\text{O})_n$ configurations for $n = 1-5$ including open chain trimer using B3LYP and PBE0 density functionals with the same aug-cc-pVDZ basis set corrected for zero point vibration energy ZPVE, hydrogen bond energy $E_{\text{H bond}}$ calculated as $(E_{\text{tot}} + \text{ZPVE}) - n(E_{\text{tot}} + \text{ZPVE})_1$, and hydrogen bond energy per bound molecule (eV).

n	B3LYP	$E_{\text{tot}} + \text{ZPVE}$	$E_{\text{H bond}}$	$1/n \cdot E_{\text{H bond}}$	PBE0	$E_{\text{tot}} + \text{ZPVE}$	$E_{\text{H bond}}$	$1/n \cdot E_{\text{H bond}}$
1		-2079.59	0.0	0.0		-2077.17	0.0	0.0
2		-4159.29	-0.11	-0.055		-4154.47	-0.13	-0.065
3		-6238.96	-0.19	-0.063		-6231.70	-0.19	-0.063
3		-6239.17	-0.40	-0.133		-6231.97	-0.46	-0.1533
4		-8319.14	-0.78	-0.195		-8309.57	-0.89	-0.2225
5		-10399.04	-1.09	-0.218		-10386.96	-1.11	-0.222

Supplementary Table S3. Observed bands in Raman spectra of H₂O and D₂O deposited in solid argon at different temperatures (cm⁻¹).

H ₂ O							D ₂ O	assignment
8K	18 K	24 K	28 K	30 K	32 K	34 K	10 K	
3726 m	3728 vw						2736 m	v ₃ monomer
3714 w								v ₃ dimer acceptor
3698 m								free OH trimer
3692 m	3691 m	3686 m	3685 m	3683 m	3681 m	3678 m		free OH tetramer, pentamer
3636 s	3636 ms	3636 mw	3637 w				2663 m	v ₁ monomer
3631 m, sh	3630 sh							v ₁ dimer acceptor
3533 mw,br	3534 vw	3534 vw	3535 w sh				2550 m	trimer donor
		3475 mw	3465 m	3468 m				cyclic trimer
3452 mw	3455 vw				3450 m	3444 m	2486 m	cyclic trimer
3410 vw	3404 vw					3413 sh		cyclic trimer
3365 vw	3374 vw			3384 sh			2446 m	cyclic hexamer
3310 vw	3304 vw		3324 mw		3306 m		2350 m	tetramer (OH) _b
3205 w	3205 vw	3196 w						pentamer (OH) _b
		3139 w	3144 mw	3120 m	3135 m	3120 m		multimers
		3086 w						multimers



Supplementary Figure S1. Left: Starting configuration for molecular dynamics simulation of 13 water molecules embedded in the face centered cubic lattice of 500 argon atoms. Right: Configuration after two simulation steps, the first at 300 K to introduce disorder and the second one at 10 K to simulate freezing. Two dimers and one open chain tetramer are visible.